Examining Conditions to Explore the Atmosphere of Uranus with Autonomous Gliders

Raymond P. LeBeau Jr.
rlebeau@slu.edu
Parks College
Saint Louis University
Saint Louis, MO 63103

Goetz Bramesfeld
bramesfeld@ryerson.ca
Ryerson University
Toronto, ON M5B 2K3
Canada

Sally Warning
swarning@slu.edu
Parks College
Saint Louis University
Saint Louis, MO 63103

Csaba Palotai
cpalotai@fit.edu
Florida Institute of Technology
Melbourne, FL 32901

Jim Dreas Justin Krofta Joe Kirwen Phillip Reyes
Parks College, Saint Louis University, Saint Louis, MO 63103

Abstract

The atmospheric dynamics of the gas giant planets of the outer solar system has been a subject of much interest since the first observations of the Great Red Spot (GRS) more than three centuries ago. In the modern era, such "spots", which are in fact large vortex features, have been seen on all four of the giant planets, along with a variety of other interesting dynamical features. Still, our view of these atmospheres is often that of surface, given that there is limited data about atmospheric changes with altitude on these planets. A key exception to this rule was the Galileo parachute probe dropped into the atmosphere of Jupiter in 1995. Galileo was followed by the ongoing Cassini-Huygens mission to Saturn, with the Huygens probe dropped into the atmosphere of Titan. A likely next target for an orbiter-atmospheric probe mission is one of the two remaining giant planets, Uranus and Neptune. This investigation considers the likely conditions to be encountered by a probe on Uranus, based on both observational data and meteorological simulations. These conditions are used to assess the potential of an autonomous glider as opposed to a parachute probe, including potential flight paths for such a mission. This analysis suggests that a glider could increase the mission duration by an order of magnitude while providing greater horizontal coverage compared to a parachute probe, significantly enhancing the mission return.

Introduction

Humanity's first and only close encounter with Uranus occurred in 1986 when the interplanetary probe Voyager 2 made its closest approach to this planet. Up to that point, Uranus was known as one of the four giant planets (along with Jupiter, Saturn, and Neptune), most notable for its extreme axial tilt, such that its rotational axis was nearly in the plane of Uranus's orbit. Voyager 2 provided much new information about this planet, including detecting thin planetary rings, discovering many moons, and providing data about wind speeds and the variation of temperature and pressure with depth at a few points in the upper atmosphere. It also captured the first detailed images of the "surface" of Uranus, or more accurately the appearance of the atmosphere at the depth where the atmosphere becomes optically thick. This revealed a light blue, nearly cloudless and featureless "cue ball" that remained the dominant image of this planet in the following decades, even as lower resolution imaging from ground-based observations and the Hubble Space Telescope were revealing a far more interesting atmosphere.

Starting in the 1990s, the next generation of probes began to revisit the gas giants. These return missions were different from the Voyager missions in two critical ways — they were designed to spend several years orbiting their target planet and they were designed to drop the first probes into these atmospheres. In 1995, the Galileo atmospheric probe parachuted into the atmosphere of Jupiter. This groundbreaking feat provided the first direct measurements of a gas giant atmosphere as a function of altitude. The Galileo probe measured the atmospheric properties both above and below the optically thick cloud deck (at about 1–2 bars of pressure for Jupiter). Functioning for just under an hour, the probe successfully measured pressure, temperature, wind speed, and chemical composition over approximately 150 km of altitude, stopping when the atmospheric pressures reached about 22 bars and the temperature was about 150 °C [1]. The next flagship mission to the gas giants, the Cassini mission to Saturn, had a similar probe (called Huygens), but it was dropped into the atmosphere of Saturn's largest moon, Titan. Thus, the Galileo probe remains the sole probe of its kind to be used in a gas giant atmosphere.

Despite the important data this probe has provided, it has also created controversy — its relatively short lifetime and vertical trajectory meant effectively a single column in the atmosphere was sampled. This left open the question of to what extent this single sounding can be used to characterize the entire atmosphere — imagine the difference in measurements if a probe were dropped over Antarctica versus the Amazon Basin on Earth. On Earth we address this problem by using many probes like weather balloons along with other remote sensing techniques at different times and locations across the planet. Unfortunately, this approach is not feasible both in terms of weight and money for gas giant exploration. An alternative is to expand the exploration envelope of the single mission to the planet. One means of achieving this is to replace the parachute probe with an autonomous aircraft which could cover more of the planet over a longer mission time. The idea of exploring other planets with remote aircraft has already been considered in a few cases. Powered aircraft missions to Mars have received a fair amount of consideration, most notably the Mars Aerial Regional-Scale Environmental Survey (ARES) project of NASA [2, 3]. Other missions are at this point more speculative, such as an aircraft with inflatable bladders exploring Titan [4] or a blimp-driven exploration of Venus [5]. While a powered aircraft might also be deployed on the gas giants, the alternative of an unpowered glider is also an attractive choice. Ideally, a slowly descending glider could provide much greater coverage in time and space compared to a parachute probe like Galileo, without some of the mechanical complexity (and possible failure points) of a powered craft.

This paper is intended to provide an initial examination of the known atmospheric conditions a potential autonomous glider would encounter in a mission to a gas giant planet as well as an initial estimate of its possible basic performance. The particular target of choice is a mission to Uranus, the next gas giant out from Saturn and arguably the next in line to receive an orbiting mission like Galileo or Cassini. In fact, such a mission is the third-highest priority flagship mission in the most recent Decadal Survey (2011, Ref. 6), which historically serves as a guidebook for future space missions. However, in contrast to terrestrial meteorological data, the collection of outer solar system data is occasional and variable; thus, Uranian meteorology is best understood in conjunction with that of the other giant planets.

Gas Giant Atmospheres

The gas giants are so named as they consist of a large amount of gaseous material with no apparent solid surface. The part of the planet that we see is the upper extent of the atmosphere with the "surface" corresponding to when the gas becomes optically thick. The atmosphere above the optically thick region is referred to as the "weather layer", in which distinct cloud, vertical spots, and other similar atmospheric features are observed. Below the "surface", the temperature and pressure gradually increase, eventually blending into what is thought to be a region of

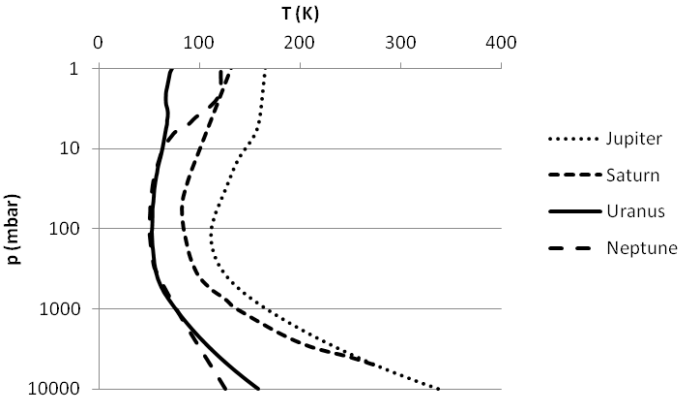

Fig. 1: Vertical temperature-pressure profiles for the four giant planets. Jupiter data taken from the Galileo probe [1]. The remaining profiles are based on occultation data with an approximate adiabatic extension below full atmospheric opacity [10–12].

strong vertical fluid convection that occupies much of the planetary interior [7]. For Jupiter and Saturn, hydrogen is thought to form the bulk of the mass of the planet, from the outer atmospheric envelope to metallic hydrogen in the interior. In the case of the outer two gas giants, Uranus and Neptune, hydrogen accounts for less than 20% of the planet mass, the hydrogen-dominated outer envelope giving way to a fluid convection region that is sometimes referred to as an icy mantle, "icy" because it is thought to be relatively rich in water, methane, and other traditionally ice-forming compounds [7]. This distinction has led to these two planets being called Ice Giants. Still, all four planets have similar upper atmospheres consisting mainly of hydrogen (80–96%) with some helium (3–20%) along with trace species like water, ammonia, ammonium hydrosulfide, and methane. For Uranus, analysis of the Voyager 2 data set the helium mole fraction at 0.15 ± 0.03 in the upper atmosphere [8], while the dominant trace species is methane with a mole fraction of around 2–3% [9].

The Galileo probe data [1] provided direct measurements of the winds and temperature with altitude down to about 20 bars. The upper portion of the thermal structure detected was largely consistent with the previous occultation studies with a tropopause at about 100 mbar and a temperature of around 110 K. Beneath this depth the atmosphere gradually approached a near-dry adiabat that persisted to the full probe depth. Only occultation techniques are available for the other giant planets, but these are only applicable above the optically thick depth of the atmosphere. At greater depths, a near-dry adiabat is conventionally assumed. This approach is used in Fig. 1, showing pressure-temperature profiles of all four giant planets.

Above this cloud deck, these atmospheres have a vertical temperature structure not dissimilar in form to Earth. All four atmospheres have distinct temperature minimums defining the top of the troposphere, all coincidentally in the vicinity of 100 mbar

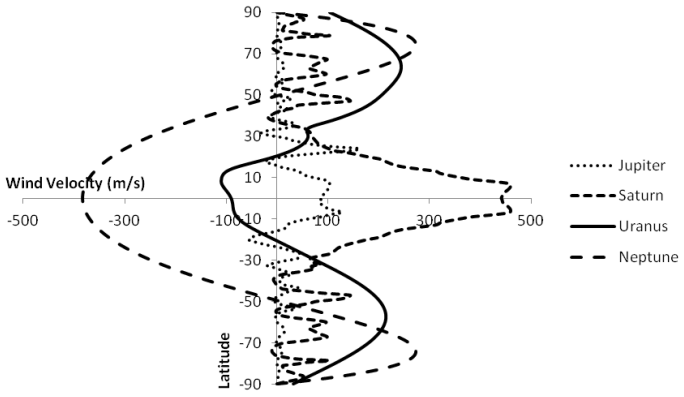

Fig. 2: Zonal wind profiles for the four gas giant planets. Positive velocity is conventionally defined as prograde (in the direction of planetary rotation). The Jupiter [13] and Saturn [14] profiles are based on binned cloud-tracking data. The Uranus [15, 16] and Neptune [17] profiles are based on curve fits to the cloud tracking data sets due to the more limited data available for the Ice Giants.

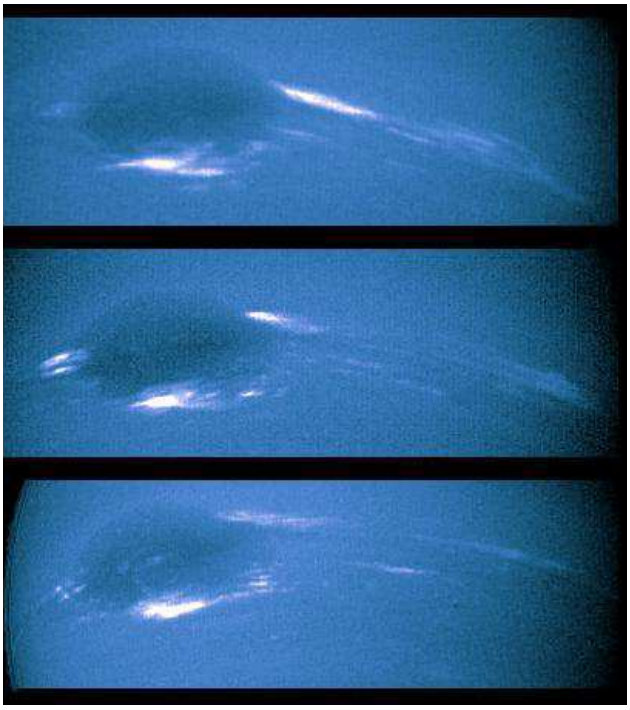

Fig. 3: Images of GDS-89 and the Bright Companion cloud (at bottom edge) on Neptune from Voyager 2 (Courtesy NASA/JPL)

(Fig. 1). The tropopause temperatures are, not surprisingly, cold, with Jupiter the warmest at about 110 K and Uranus and Neptune the coldest at around 50 K. Above this level, the temperature rises with height like the stratosphere on Earth. Below this level, the temperature increases with depth like in Earth's troposphere, eventually approaching an adiabatic lapse rate as the optically thick "surface" is reached between one and four bars of pressure. Based on theory, this adiabatic lapse rate region is expected to extend inward to depths corresponding to many tens of bars of pressure, an assumption that proved at least not inconsistent with the Galileo probe measurement.

The wind fields of these atmospheres are primarily determined by cloud-tracking, using either spacecraft or telescope images. This process for Uranus is described in Sromovsky et al. [18], but similar processes have been applied to all the giant planets. The result is a zonal wind variation with latitude for the "weather layer" or upper troposphere where isolated cloud features can be tracked. Based on these observations, all the giant planet atmospheres have strong, persistent zonal jets similar to Earth's jet streams. However, unlike Earth where the jet streams must weave between colliding high and low pressure systems, the larger surface area of the gas giants gives plenty of room, allowing the jet winds to travel with minimal north-south deviations from the dominant east-west motion. On Jupiter and Saturn, the zonal winds have numerous peaks with prograde jets at the equator; on Uranus and Neptune, there are only a few peaks and the equatorial jet winds are retrograde (Fig. 2). These jets achieve velocities of hundreds of meters per second, with maximum velocities on Saturn and Neptune of around 400 m/s.

Also like Earth, the giant planet atmospheres have large vortex structures, often called "spots". While often analogized to hurricanes, the majority are actually more akin to high pressure systems. The first discovered, longest-lasting, and best-known of these large vortices is the Great Red Spot (GRS) of Jupiter, a large high pressure system that may have persisted for more than four centuries. In the modern era, large vortex features have been seen on all four of the giant planets. While in general these features have not had the apparent longevity of the GRS, many exist for months or years. One notable example is the original Great Dark Spot (GDS-89) of Neptune, closely observed by Voyager 2 in 1989. This vortex exhibited a variety of dynamics, including periodic shape oscillations and a long-term equatorward drift. It also was accompanied by a large bright methane cloud feature dubbed the Bright Companion (BC) throughout these motions (Fig. 3). Other notable vortices include the three White Ovals that merged into a single vortex on Jupiter, the Northern Great Dark Spots on Neptune [19], and most recently the Uranian Dark Spot (UDS) [16]. In general, these features like the distinct cloud features are thought to be located in the upper troposphere, from about 100 mbar down to a few bars of pressure. A common explanation for the companion clouds is that they are orographic, forming as the atmosphere moves up and over the vortex [20]. Such regions of upwelling are of interest to a potential gliding mission, but direct observations of these vertical motions are not currently possible. However, atmospheric models based on known observations can provide some further insight into these weather conditions.

Atmospheric Modeling

While the basic motions of gas giant atmospheres are defined by the observational record, for the flight of a small aircraft one would prefer more detailed information about atmospheric conditions. In particular for a gliding flight, regions of sufficiently strong upward motion could serve to significantly extend the potential mission. While there have not been direct observations of strong updrafting on Uranus, simulations have indicated in the vicinity of dark spots there may be regions of relatively strong updrafts and downdrafts. A review of these results is presented here to illustrate this possible consideration in designing a gliding mission on Uranus.

There are several different atmospheric models used for the giant planets, but the "weather layer" of the Ice Giants has been most extensively studied with the Explicit Planetary Isentropic Coordinate General Circulation Model (EPIC GCM) [21]. EPIC is a finite-difference solver designed to solve the dynamics of gas giants atmospheres based on an initial wind structure, vertical temperature-pressure profile, and distribution of important trace gases. The numerics of the EPIC GCM are described in multiple references [21,22] and are based off the meteorological model of Hsu and Arakawa [23], The model solves the three-dimensional Navier-Stokes equations on an oblate spheroid, the horizontal dimensions being defined by a grid of latitude and longitude. The vertical coordinate is a hybrid potential temperature-pressure coordinate, ζ, following Konor and Arakawa [24] and defined in EPIC as

$$\zeta = f(\sigma) + g(\sigma)\theta, \qquad \sigma = \frac{\log(p/p_{\text{bot}})}{\log(p_{\text{top}}/p_{\text{bot}})}$$

where θ is the potential temperature and p is the pressure, with the pressures at the top and bottom boundaries specified. The functions $f(\sigma)$ and $g(\sigma)$ are defined as appropriate for the problem ($g(\sigma)$ approaching zero near solid surfaces, $f(\sigma)$ approaching zero and $g(\sigma)$ approaching unity when purely isentropic coordinates are desired). Simulation of methane microphysics is based on the advection of trace gases combined with the parameterization of phase change processes as described in Ref. 25, adopted for methane as described in Ref. 26.

Previous Ice Giant studies using EPIC have included the dynamic motions of GDS-89 [27,28], the formation of companion clouds [20,29], and the stability of the UDS [16]. These inputs are constrained to the extent possible by known observational data, and the subsequent simulation is likewise evaluated against observational data. Vertically, the simulations generally extend from a few millibars down to 5–10 bar, while horizontally they can range from specified bands of latitude to the entire globe.

Inputs to the simulations include the zonal wind profile, the vertical temperature-pressure profile, and initial average relative humidity based on observed data and related theory. Of these inputs, one that has been repeatedly redefined in the past two decades is the zonal wind profile. Uranus's initial zonal wind profile was not as well-constrained as the other gas giants due to there being few cloud features to track during the Voyager 2 encounter. As more observational data has been obtained, new profiles have been developed; meaning there is no single established zonal wind profile for Uranus [18]. As Uranus also possesses the most extreme seasonal changes (due to its near-horizontal axial tilt), there is ongoing debate as to whether the zonal profile may be experiencing seasonal changes as well. As tested in Ref. 16, the profile from the Sromovsky and Fry fit of cloud drift rate [15] can be modified to create a latitude band of more uniform absolute vorticity gradient while still largely conforming to the observational data. Near-uniform gradient regions in potential vorticity have proven critical for achieving coherent, meridionally drifting vortices while regions of near-zero gradients have been critical to achieve clear periodic shape oscillations like those seen in GDS-89 [26, 27]. Such a profile is shown for Uranus in Fig. 2, with the region of zero potential vorticity gradient at around 30 degrees north latitude. This profile is therefore convenient for vortex-companion cloud simulations. The pressure-temperature profiles (Table 1) and methane humidity value are based on the observational data. Further details of these simulation parameters may be found in Refs. 26, 29 and 30.

Table 1: Sample atmosphere layer setup for a 13-layer model of Uranus

Layer	ζ [K]	p [mbar]	T [K]	θ [K]
1	597.5	4.85622E+00	70.8	597.5
2	334.5	1.67952E+01	65.1	334.5
3	180.7	5.87585E+01	59.4	184.6
4	98.8	1.11704E+02	52.8	126.9
5	95.0	1.52502E+02	53.1	112.7
6	91.3	2.08197E+02	54.0	101.3
7	87.5	2.84239E+02	55.5	91.9
8	83.7	3.88055E+02	58.1	84.8
9	80.0	5.29786E+02	62.3	80.3
10	74.0	8.69883E+02	72.9	77.3
11	66.5	1.62154E+03	89.7	74.5
12	59.0	3.02235E+03	109.7	72.0
13	51.5	5.63325E+03	133.2	69.7

The methane cloud microphysics model for this simulation advects humidity and allows for phase changes from vapor to ice cloud particles. The output of these simulations include the time-accurate evolution of velocity and vorticity fields, the distribution of trace gases and clouds, and in the case of vortices the evolution of the vortex structure. As such, these simulations provide a database that can be used to provide an initial evaluation of conditions for gliding flight. A sample of these results is provided in Fig. 4, in this case the evolution of a UDS-like vortex and a bright methane cloud companion. The vortex is defined

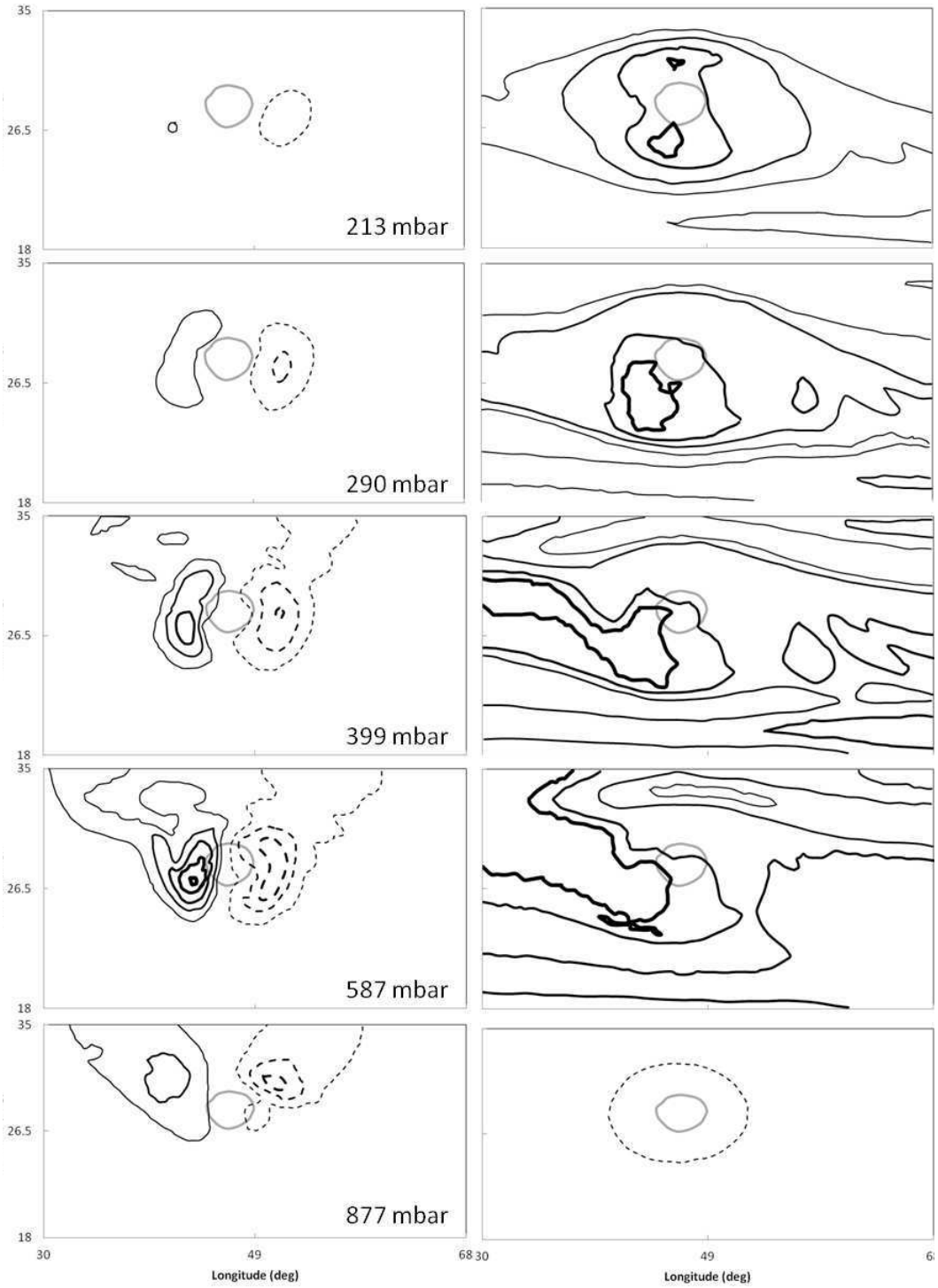

Fig. 4: Results of 50 day simulation of a dark spot on Uranus, revealing a region of upwelling along the leading edge. Five different pressure layers are shown, with the vortex itself centered at 750 mbar. The horizontal extent of the vortex is shown as a positioning reference in all layers as a grey ellipse. The left column shows vertical velocity, with solid contours indicating regions of upward velocity and dashed contours downward, the thinnest contours representing magnitudes of 1 cm/s and subsequent contours set-off with a spacing of 1 cm/s. On the right is the corresponding distribution of methane humidity, from the thickest contours at 100% (clouds) down to 65% for the thinnest. The bottom layer shows a dashed contour of 50% relative humidity, indicating the layers below the vortex act as a methane source since the initial assumed RH in all layers for this simulation is 60%. The strong upwelling seen in the 399 and 587 mbar layers produces the cloud region seen at 587 mbar and above.

by a closed contour of constant potential vorticity (which corresponds to a material surface), the cloud by a contour of 100% relative humidity. The cloud identifies a region of upwelling as the background air is pushed over the vortex. This type of atmospheric uplift phenomena is not unique to the Ice Giants — it is similar to orographic uplift over mountain ranges (which also can lead to clouds) or the ageostrophic motion associated with the divergence of the Q vector in the vicinity of high and low pressure systems [31]. Note that the rotational directions on Uranus are flipped relative to Earth, since the dynamical North Pole corresponds to the South Pole of Uranus as defined by the International Astronomical Union. This means that the high pressure spot is rotating counter-clockwise despite being located in the northern hemisphere.

Analyses of the conditions near the Great Red Spot both from observational data [32] and simulations [33] have yielded vertical wind estimates of 1–4 cm/s on Jupiter. On Uranus, the resulting maximum velocities of these updrafts based on simulations like that shown in Fig. 4 are comparable at less than 10 cm/s. As there is no data directly measuring vertical wind motion in the Uranian atmosphere, these simulations are currently the strongest evidence of updrafts in the upper troposphere of Uranus. Thus, this serves as an upper bound for the glider flight performance study.

Potential Glider Missions

Based on the atmospheric conditions, flight on Uranus is in many ways less far-fetched than the already proposed flight on Mars with conditions much more similar to those on Earth. The gravitational acceleration of Uranus at its "surface" is about 10% less than that of Earth at 8.69 m/s^2, with Uranus's comparatively larger mass being balanced by a larger radius. In the upper troposphere, the pressure and densities are also not comparable to Earth. The tropopause is at a pressure of about 100 mbar with a density of around 0.05 kg/m^3 (Fig. 5). Moving down to 1 bar in pressure, the density increases to 0.38 kg/m^3, or roughly one-third Earth sea level conditions, and at 20 bar, the density approaches 3 kg/m^3. The combination of the density and gravitational acceleration suggest that in much of the troposphere conventional or gliding flight should be achievable. As already discussed, atmospheric models even suggest the possibilities of soaring flight using thermals and ridge-lift like occurrences. The big difference compared to Earth is the temperature, which runs from 50–55 K at the tropopause to about 75 K at 1 bar, rising to around 190 K at 20 bar. However, the Huygens probe passed through temperatures of 70–100 K, which suggests that these temperatures do not represent an insurmountable challenge.

Of the possible craft that might be used to investigate the atmosphere of Uranus in situ, a glider is an attractive option. An autonomous glider would significantly increase the flight time and range over a traditional parachute probe such as Galileo or Huygens. In contrast, a powered aircraft would need to bring along its own oxidizer at minimum, since there is little oxygen in the Uranian atmosphere. While transporting oxidizer is conceivable, a significant weight penalty results from its higher molecular weight and additional support equipment, such as that required to maintain a liquefied state of the oxidizer. Alternative powered flight propulsion concepts, such as nuclear based propulsion, also present an increase in system complexity and the likelihood of mission failure. Especially considering the demanding conditions during the spacecraft launch and a lengthy interstellar transition in the order of 10 years, the simplicity of a glider is appealing. Furthermore, a glider also can take advantage of any atmospheric lifting mechanisms, such as "ridge lift" in the vicinity of vortices, thermals, or similar uplift phenomena that may exist in the atmosphere, thus potentially resulting in flight times exceeding those of powered flight concepts.

Potential Glider Designs

The purpose of this design study of a Uranus glider is to provide a starting point for conceiving possible science missions. Rather than providing an optimized final design, the goal is to identify challenges and opportunities. The subsequent findings will help to develop potential science missions, that in turn will lead to further conceptual studies of the flight vehicle and science mission. In summary, the herein introduced glider designs form a basis for assessing the feasibility of using gliders for science missions on Uranus.

The potential performance of a gliding probe hinges on the design of the glider. As there have been no Uranus gliders to

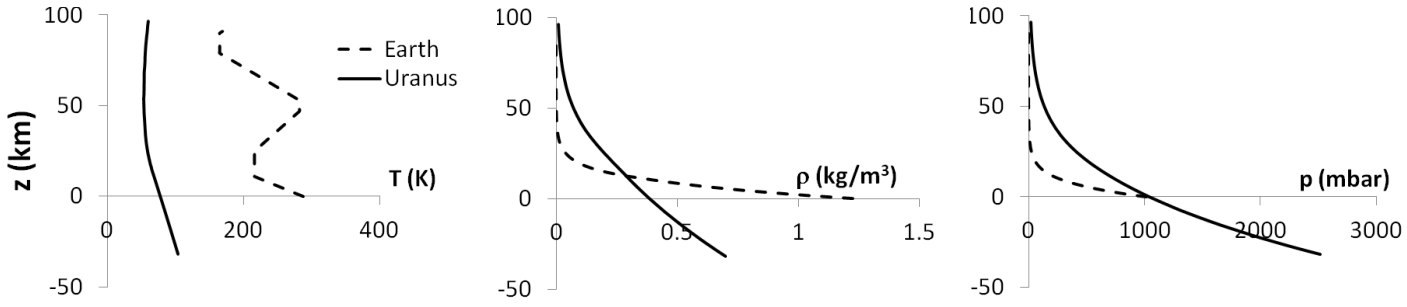

Fig. 5: Comparisons of the temperature (left), density (center), and pressure (right) profiles of the atmosphere of Uranus and a standard Earth atmosphere. Altitude is arbitrarily fixed to be zero at one bar of pressure for both atmospheres.

Table 2: Atmospheric conditions during gliding flight conditions on Uranus

p	T	ρ	a	μ	ν	V_{TAS}	M	Re/l
[bar]	[K]	[kg/m^3]	[m/s]	[Ns/m^2]	[m^2/s]	[m/s]	[–]	[1/m]
0.1	54	0.098	543.3019	2.24E-06	2.29E-05	73.40133	0.135102	3.21E+06
1	76	0.364	644.5419	3.20E-06	8.79E-06	38.08608	0.05909	4.33E+06
20	193	2.878	1027.124	7.21E-06	2.51E-06	13.54477	0.013187	5.41E+06

date, the appropriate design is speculative. As such, terrestrial gliders and other previous planetary missions provide reasonable sets of parameters. Using these guidelines, several different aircraft designs were considered, of which two are introduced: a larger, Earth-like glider and a smaller design that was based on the Mars ARES project. The two designs discussed in this section represent first explorations of the design space and an entry point for the planning of any science missions using gliding probes on Uranus.

For a starting point in the conceptual design process, the aerodynamic conditions on Uranus are estimated using Earth-based gliders [34] and are summarized in Table 2. The values are based on a typical club-class glider with a wing loading of approximately 260 N/m^2 and operating at a lift coefficient of 1.0. Flight speeds are of similar magnitude as encountered on earth and the flight regime is essentially incompressible with Mach numbers ranging from about 0.14 near the tropopause to nearly 0.013 at 20 bar. The respective 1-metre chord Reynolds numbers range from about $3.2 \cdot 10^6$ to nearly $5.4 \cdot 10^6$, which is about two to three times the value typical for Earthly glider.

The two glider designs were analyzed using a drag decomposition. Induced drag was predicted using a potential flow approach and profile drag using tabulated section data, which was computed using XFOIL [35]. Empennage drag was determined in a similar manner. In addition, the incidence angle of the horizontal tail was adjusted in order to trim the aircraft with static margins of approximately 10% of the mean aerodynamic chord. Fuselage drag was estimated using its wetted surface area. An additional 10% interference drag was assumed for each velocity point that was analyzed. The drag over the velocity range was computed for three different altitudes (0.2, 1.0, and 20 bar) in order to capture any Reynolds number effects.

The wings of both designs are equipped with an NLF 0416 airfoil [36] and the empennages with an NACA 0012 airfoil. Ultimately, these airfoils are likely to be suboptimal for a Uranus mission and were primarily chosen as place holders based on their design chord Reynolds numbers, which are similar to those expected during flight on Uranus. Without going too much into further details, an airfoil designed specifically for a Uranus mission probably has a more relaxed maximum lift coefficient and a smaller low-drag region with lower profile drag coefficients than the NLF 0416. Such an airfoil has to reflect the fact that the Uranus glider is "dropped" into the atmosphere without any significant launch and landing requirements and that it primarily operates at a single angle of attack. Specifics, however, will have to be subject of future studies once the science missions are better defined.

Large Uranus Glider

The larger glider has an estimated wingspan of 12 m. The root chord is about 1.2 m, a tip chord about 0.4 m. The total wing area is 9.6 m^2. The overall fuselage length is 5.5 with a maximum cross section for the science bay of 1.1×0.4 m. As shown in Fig. 6, the glider fits within the space of the existing

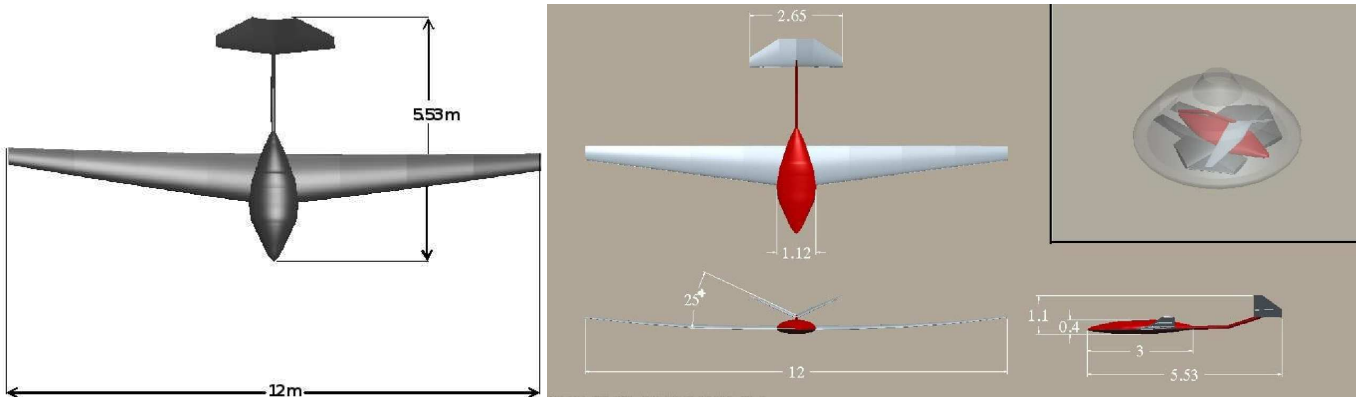

Fig. 6: Schematic of the larger aircraft design in flight (left) and packaged into the equivalent of the MSL entry capsule (right).

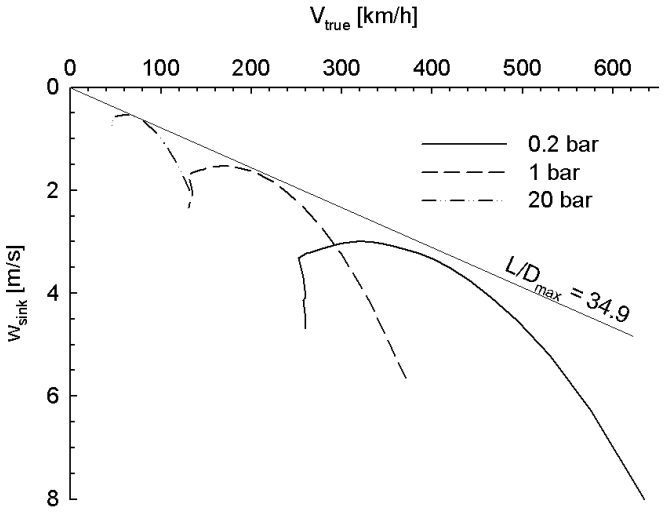

Fig. 7: Predicted speed polars of large Uranus glider design for three different altitudes

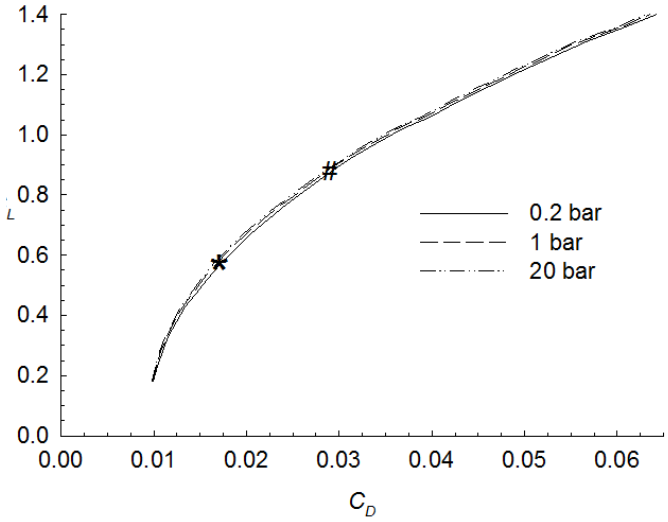

Fig. 8: Predicted performance of large Uranus glider design in coefficient form for three different altitudes (* best glide and # best endurance conditions)

entry vehicle of the Mars Science Laboratory, which has an interior space of 3.7 m diameter and a height of 1.2 m. This requires the wing being folded four times and the fuselage once. The unfolding sequence is automated and adapted from other planetary flight mission concepts. Nevertheless, the folding mechanisms add complexity and weight to the overall system.

The total flight mass of the large design is 380 kg that is comparable to that of the Galileo and Huygens probes. The individual mass contributions are listed in Table 3. Wing and fuselage weights were estimated using data of Earth gliders [34] and include about 10% weight penalty for each folding hinge and mechanism. The scientific instrumentation of the Galileo probe includes an atmospheric structure instrument, a neutral mass spectrometer, a nephlometer, a net flux radiometer, and a helium abundance detector. With this package, the probe is able to measure pressure, temperature, density, molecular weight, chemical composition, cloud structure, thermal energy profiles, and wind speeds. The mass of this scientific payload is about 25 kg. It is assumed that power is provided by a Radioisotope Thermoelectric Generator (RTG), similar to that used on the Galileo and Mars Curiosity missions. Based on these previous missions, it is expected that the RTG is about 45 kg and will also provide sufficient excess heat to keep the instrumentation at functional temperatures. Additional payload weights include the communication system and guidance, navigation, and control.

The predicted flight performance of the large Uranus glider design is shown in Figs. 7 and 8. As expected the best glide ratio improves slightly from about 33.4 to 34.9 as the glider descends and the kinematic viscosity results in increasing chord Reynolds numbers. At the same time the true airspeed decreases for a given angle of attack. The sink rates and forward flight speeds are comparable to those encountered on Earth, especially at the lower altitudes of 1 and 20 bar. The lift and drag coefficients for best glide and best endurance are very similar since Reynolds number effects are limited.

Table 3: Mass breakdown of large Uranus glider design (Aircraft 1)

System	Mass (kg)
Science Payload	25
RTG	45
Other Fuselage/Payload	90
Wing	180
Tail and Empennage	40
Total	380

Small Uranus Glider

The lighter glider design is a scaled down version of the first one with a 6 m wingspan comparable to that of the Mars ARES design and a wing area of 4.8 m^2. The flight mass is 125 kg, which is comparable to that of the Mars Ares design minus the propulsion system and propellant. This aircraft is intended to represent a smaller-scale mission, presumably with a scaled down scientific payload, which has reduced weight and complexity due having only two wing folds and one fuselage fold.

The glide sink polars and lift versus drag coefficient plots of three different altitudes are listed in Figs. 9 and 10, respectively. Similar to the large Uranus glider design, Reynolds number effects are small — the best glide ratio varies from about 22.4 to 23.1 over the expected pressure altitude range from 0.2 bar to 20 bar. The lift coefficients corresponding to maximum range

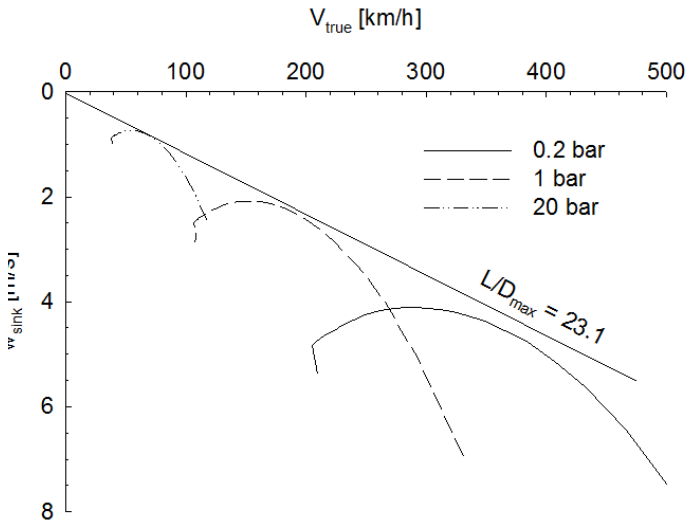

Fig. 9: Predicted speed polars of small Uranus glider design for three different altitudes.

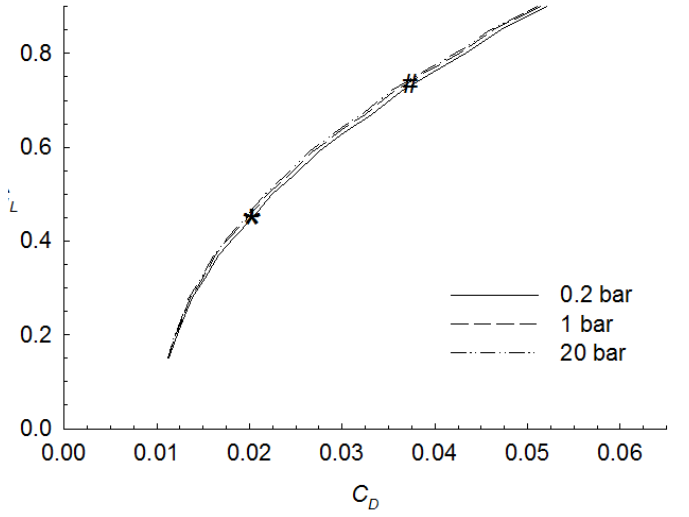

Fig. 10: Predicted performance of small Uranus glider design in coefficient form for three different altitudes (* best glide and # best endurance conditions)

and endurance are smaller than what one is used to from Earthly gliders. For instance the maximum lift-to-drag ratio of the small Uranus glider is at C_L= 0.45 compared to about 0.8 for a typical standard class glider. A similar trend can be observed for the large Uranus glider design, C_L= 0.57. These differences in lift coefficients related to performance maxima is primarily due to smaller fuselages in relation to the wing sizes of the Uranus gliders than typical for Earth gliders. Subsequently, the wing drag becomes more dominant for the Uranus gliders.

Table 4: Values used for gliding flight analysis

	Large Uranus Glider	Small Uranus Glider
C_L for max endurance	0.87	0.72
$C_L^{3/2} \Big/ C_D$ for max endurance	28.7	17.1
C_L for $(L/D)_{\max}$	0.57	0.45
$(L/D)_{\max}$	34.4	22.9

Atmospheric Entry

The mission assumes a shielded entry vehicle that carries the glider before it is released into the atmosphere. Initially slowed by atmospheric friction, at some point a parachute will deploy and further slow the descent. The glider deploys once the entry vehicle has descended to a pressure altitude of 0.2 bar. At this point the payload instruments and communication system, as well as the UAV's control systems are fully operational. While the instruments collect data, the control actuators correct the orientation and flight path of the UAV. The aircraft glides between pressures of 0.2 bar to 20 bar, which corresponds to an altitude band of 170 km. During the gliding phase, the glider relays its atmospheric measurements to the orbiter in manner similar to the Huygens and Galileo probes. For that purpose the control systems has to stabilize the vehicle and maintain the communication link by keeping the aircraft's antenna in the proper orientation, along with guiding it along the desired flight path. The UAV is not expected to survive below a pressure altitude of 20 bar due to a number of factors, including structural damage from the pressure or temperature, inability to transmit through the dense atmosphere at this depth, or power failure. This will conclude the UAV's mission, though the orbiter's observational mission wuld presumably continue.

Flight Mission

The large Uranus glider has a maximum endurance of about 50 hours and a maximum range of about 5800 km and the respective values of the small Uranus are almost 37 hours and 3800 km. Even at best range conditions the large glider flies for about 46 hours and the small glider for about 32 hours. The performance of the gliding portion of the Uranus mission was analyzed using the predicted performance presented in Figs. 8 and 10. A maximum range without wind and maximum endurance mission were considered. Due to the small Reynolds number effects, the conditions at 1 bar were assumed over the entire gliding flight using the values listed in Table 4. The analysis assumes flight at a constant angle of attack, and thus constant lift coefficient. This requires an adjustment of the true airspeed as the density changes during descend form 0.1 bar to 20 bar which is an altitude of approximately 170 km. The maximum range, $D_{\max}$, is simply computed using the usable altitude, h,

Table 5: Comparison of Galileo and Huygens probe missions to proposed Uranus UAV mission.

Probe	Destination	Arrival	Payload Mass [kg]	Total Mass [kg]	Pressure Range [bar]	Descent [km]	Duration [hrs]	Cause of mission termination	Total Mission Cost
Galileo	Jupiter	Dec, 1995	24.1	339	0.45–23	167	1	Temperatures at 23 bar cause transmitter failure	$1.5 billion
Huygens	Titan	Jan, 2005	49.0	349	0.003–1.6	160	2.5	Battery depletion	$3.3 billion
Uranus UAV	Uranus	—	25	380	0.2–20	170	50	—	—

and the maximum lift-to-drag value:

$$D_{\max} = h \cdot (L/D)_{\max}$$

Maximum endurance, $t_{\max}$, is given by:

$$\begin{aligned} t_{\max} &= h\sqrt{\frac{\rho S}{2W}}\left(\frac{C_L^{3/2}}{C_D}\right)_{\max} \\ &= \sum \Delta h \sqrt{\rho_{\text{avg}}}\sqrt{\frac{S}{2W}}\left(\frac{C_L^{3/2}}{C_D}\right)_{\max} \end{aligned}$$

In order to account for the changing density as the glide descends, endurance is computed by adding the time increments that the glider requires to descend through an altitude band, Δh, which has the average density ρ_{avg}.

Straight flight may not be a desirable mission. At its maximum range of 5800 km the large glider can cover about 10 degrees in latitude without accounting for any wind. Considering that zonal winds on Uranus reach velocities of 200 m/s (about 1000 km/h) relative to the planetary rotation other flight profiles may be more advantageous than the best glide speeds. For example depending on the science mission, a cross-wind dash or a downwind mission with the proper speeds-to-fly have to be considered. The downwind dash, for example, would be optimized by flying close to maximum endurance speed. In addition, the flight path may be extended by taking advantage of regions of atmospheric uplifts that enable autonomous soaring and gust soaring similar to those approaches described by Edwards and Silberberg [37] or Langelaan [38]. One possible mission is to locate a region of ridge lift associated with a vortex and slowly descend in a roughly circular path with a radius of tens or hundreds of kilometers. Another promising mission profile is for the aircraft to seek out regions of maximum uplift and reside in them for a period of time. Given our limited understanding of the atmospheric conditions, these proposed paths of any mission serve more as a guideline than a fixed track that can enhance any potential science mission. Despite these uncertainties in planning, the value of the glider over a simple drop probe is the glider's ability to obtain data over a larger area and longer time period than that achievable by a parachute probe.

Discussion

The concept of an autonomous gliding flight with a buoyancy-driven glider has been explored in Ref. 4 as a possible means of investigating the atmosphere of Titan. Here, we have considered a similar glider mission on Uranus. A comparison of the parachute probe missions to Jupiter and Titan and the current theoretical mission to Uranus is shown in Table 5. A glider mission clearly has the potential to generate a longer residence time along with the possibility of a controlled exploration across a sizeable horizontal section of the atmosphere. While the regions of vertical uplift simulated in the upper troposphere to date are not enough to dramatically extend the mission, further observations and simulations at higher resolutions may reveal stronger, concentrated regions that could significantly increase the flight time. With the assistance of meteorological modeling, potential missions could be mapped out in advance of the launch and the autopilot tuned to likely atmospheric conditions. The successful use of an autonomous glider could open a new avenue of planetary exploration that would greatly expand our understanding of the differing atmospheres within our solar system.

Conclusions

In a feasibility study glide concepts were explored as alternative options for the exploration of the atmosphere of Uranus. In comparison to a simple parachuted drop probes, the glider concepts can operate at least 20 times or longer than a parachute probe with a similar science payload. The glider can further extend the exploration by exploiting possible atmospheric lifting mechanisms, such as thermals and updrafts ahead of vortex systems. Depending on the needs of the science mission, the glider can explore the planet along its latitudes, towards the poles, or at stationary location. Further details have to be decided with the planning of the science mission, which, ultimately, will also drive a more optimized glider design.

Acknowledgments

This work was supported by NASA Planetary Atmospheres Grant No. NNX11AC01G.

References

[1] Seiff, A. et al., "Thermal structure of Jupiter's atmosphere near the edge of a 5-μ Hot Spot in the North Equatorial Belt," *Journal of Geophysical Research*, Vol. 103, No. E10, 1998, pp. 22857–22889.

[2] Dufresne, S., Johnson, C., and Mavris, D. M., "Variable Fidelity Conceptual design Environment for Revolutionary Unmanned Aerial Vehicles," *Journal of Aircraft*, Vol. 45, No. 4, 2008, pp. 1410–1412.

[3] Kuhl, C. A., "Design of a Mars Airplane Propulsion System for the Aerial Regional-Scale Environmental Survey (ARES) Mission Concept," Report TM-2009-215700, NASA, 2009.

[4] Morrow, M., Woolsey, C. A., and Hagerman, G., "Exploring Titan with autonomous, buoyancy-driven gliders," *Journal of the British Interplanetary Society*, Vol. 59, No. 1, 2006, pp. 27–34.

[5] Colozza, A. J., "Radioisotope Stirling Engine Powered Airship for Low Altitude Operation on Venus," Report CR-2012-217665, NASA, 2012.

[6] Committee on the Planetary Science Decadal Survey, Space Studies Board Division on Engineering and Physical Sciences, National Research Council of the National Academies, *Vision and Voyages for Planetary Science in the Decade 2013-2022*, National Academies Press, Washington, DC, 2011.

[7] Guillot, T., "The interiors of giant planets: Models and outstanding questions," *Annual Review of Earth and Planetary Sciences*, Vol. 33, 2005, pp. 493–530.

[8] Conrath, B., Gautier, D., Hanel, R., Lindal, G., and Marten, A., "The Helium Abundance of Uranus from Voyager Measurements," *Journal of Geomphysical Research*, Vol. 92, No. A13, 1987, pp. 15003–15010.

[9] Lunine, J. I., "The Atmospheres of Uranus and Neptune," *Annual Review of Astronomy and Astrophysics*, Vol. 31, 1993, pp. 217–263.

[10] Conrath, B. J., Gautier, D., Hanel, R. A., and Hornstein, J. S., "The helium abundance of Saturn from Voyager measurements," *Astrophysical J.*, Vol. 282, July 1984, pp. 807–815.

[11] Lindal, G. F., Lyons, J. R., Sweetnam, D. N., Eshelman, V. R., and Hinson, D. P., "The atmosphere of Uranus: Results of the radio occultation measurements with Voyager 2," *J. Geophysical Research*, Vol. 92, December 1987, pp. 14987–15001.

[12] Conrath, B. J., Gautier, D., Lindal, G. F., Samuelson, R. E., and Shaffer, W. A., "The helium abundance of Neptune from Voyager measurements," *J. Geophysical Research*, Vol. 96, October 1991, pp. 18907–18919.

[13] Limaye, S. S., "Jupiter: New estimates of the mean zonal flow at the cloud level," *Icarus*, Vol. 65, No. 2–3, March 1986, pp. 335–352.

[14] Sánchez-Lavega, A., Rojas, J. F., and Sada, P. V., "Saturn's Zonal Winds at Cloud Level," *Icarus*, Vol. 147, No. 2, October 2000, pp. 405–420.

[15] Sromovsky and Fry, "Dynamics of cloud features on Uranus," *Icarus*, Vol. 179, No. 2, December 2005, pp. 459–484.

[16] Hammel, H. B. et al., "The Dark Spot in the Atmosphere of Uranus in 2006: Discovery, Description, and Dynamical Simulations," *Icarus*, Vol. 201, No. 1, May 2009, pp. 257–271.

[17] Sromovsky, L. a., Limaye, S. S., and Fry, P. M., "Dynamics of Neptune's major cloud features," *Icarus*, Vol. 105, No. 1, September 1993, pp. 110–141.

[18] Sromovsky, L. A., Fry, P. M., Hammel, H. B., de Pater, I., and Rages, K. A., "Post-equinox dynamics and polar cloud structure on Uranus," *Icarus*, Vol. 220, No. 2, August 2012, pp. 694–712.

[19] Sromovsky, L. A., Fry, P. M., and Baines, K. H., "The unusual dynamics of northern dark spots on Neptune," *Icarus*, Vol. 156, No. 1, March 2002, pp. 16–36.

[20] Stratman, P. S., Showman, A. P., Dowling, T. E., and Sromovsky, L. A., "EPIC simulations of bright companions to Neptune's great dark spots," *Icarus*, Vol. 151, No. 2, June 2001, pp. 275–285.

[21] Dowling, T. E. et al., "The EPIC Atmospheric Model with an Isentropic/Terrain-Following Hybrid Vertical Coordinate," *Icarus*, Vol. 182, No. 1, May 2006, pp. 258–273.

[22] Dowling, T. E. et al., "The Explicit Planetary Isentropic-Coordinate (EPIC) atmospheric model," *Icarus*, Vol. 132, No. 2, April 1998, pp. 221–238.

[23] Hsu, Y.-J. G. and Arakawa, A., "Numerical modeling of the atmosphere with an isentropic vertical coordinate," *Monthly Weather Rev.*, Vol. 118, No. 10, October 1990, pp. 1933–1959.

[24] Konor, C. S. and Arakawa, A., "Design of an atmospheric model based on a generalized vertical coordinate," *Monthly Weather Rev.*, Vol. 125, No. 7, July 1997, pp. 1649–1673.

[25] Palotai, C. and Dowling, T. E., "Addition of water and ammonia cloud microphysics to the EPIC model," *Icarus*, Vol. 194, No. 1, March 2008, pp. 303–326.

[26] Deng, X., LeBeau Jr., R. P., and Palotai, C., "Numerical Investigation of Orographic Cloud and Vortex Dynamics on the Ice Giant Planets," *AIAA 1st Atmospheric & Space Environments Conference*, San Antonio, June 22–25 2009, AIAA-2009-3643.

[27] LeBeau Jr., R. P. and Dowling, T. E., "EPIC Simulations of Time-Dependent, Three-Dimensional Vortices with Application to Neptune's Great Dark Spot," *Icarus*, Vol. 132, No. 2, April 1998, pp. 239–265.

[28] Deng, X. and LeBeau Jr., R. P., "Comparative CFD Simulations of the Dark Spots of Uranus and Neptune," *AIAA 37th Fluid Dynamics Conference and Exhibit*, AIAA, Miami, FL, June 25–28 2007, AIAA-2007-3973.

[29] LeBeau Jr., R. P., Warning, S. W., and Palotai, C., "Orographic Cloud Development Paired With Atmospheric Vortex Dynamics on Uranus and Neptune," *3rd AIAA Atmospheric & Space Env. Conf.*, Honolulu, Hawaii, June 27–30 2011, AIAA-2011-3202.

[30] Warning, S. W., LeBeau Jr., R. P., Palotai, C., and Deng, X., "Effects of Hemispheric Circulation on Uranian Atmospheric Dynamics and Methane Depletion," *4th AIAA Atmospheric and Space Environments Conference*, New Orleans, LA, June 25–28 2012, AIAA-2012-2931.

[31] Holton, J. R., *An introduction to dynamics meteorology*, International Geophysics (Book 88), Elsevier Academic Press, Burlington, MA, 4th ed., April 2004.

[32] Read, P. L., Gierasch, P. J., Conrath, B. J., and Yamazaki, Y. H., "3D balanced winds and dynamics in Jupiter's atmosphere from combined imaging and infrared observations," *Advances in Space Research*, Vol. 36, No. 11, 2005, pp. 2187–2193.

[33] Morales-Juberías, R. and Dowling, T. E., "Jupiter's Great Red Spot: Fine-scale matches of model vorticity to prevailing cloud patterns," *Icarus*, Vol. 225, No. 1, July 2013, pp. 216–227.

[34] Thomas, F., *Fundamentals of Sailplane Design*, College Park Press, Silver Spring, Maryland USA, 1999.

[35] Drela, M., "XFOIL: An Analysis and Design System for Low Reynolds Number Airfoils," *Low Reynolds Number Aerodynamics*, edited by T. Müller, Vol. 54 of *Lecture Notes in Engineering*, Springer Berlin Heidelberg, 1989, pp. 1–12.

[36] Somers, D. M., "Design and Experimental Results for a Natural-Laminar-Flow Airfoil for General Aviation Applications," Technical Paper 1861, NASA, June 1981.

[37] Edwards, D. and Silberberg, L., "Autonomous Soaring: The Montague Cross-Country Challenge," *Journal of Aircraft*, Vol. 47, No. 5, 2010.

[38] Langelaan, J. W., "A Gust Soaring Controller for Small Uninhabited Gliders," *Technical Soaring*, Vol. 35, No. 2, April–June 2011, pp. 48–60.